

Data Interaction-based Sintering Process Modeling and Online Tumble Strength Monitoring for Digital Twin System

Xuda Ding, Jiale Ye, Wei Liu, Cailian Chen, Xinping Guan

Abstract—Digital twin (DT) techniques enable the virtual model to interact with the physical process long term, showing the potential for accurate online modeling and monitoring. However, constructing an accurate sintering process model with data interaction and monitoring online tumble strength (TS) in DT is difficult because i) The complex thermo-chemical process, and the non-uniformity of materials in the sintering process make constructing a suitable data-driven model scheme with data interaction difficult; ii) Designing a data-driven model to be flexible to the time-varying sintering process with low computing complexity, and further guarantees the continuous output in DT is challenging; iii) The data from the sintering process is incomplete and insufficient for constructing a data-driven model directly, which will cause an inaccurate model. This paper addresses these challenges and constructs a novel light-weighted data-driven TS model. Specifically, a multi-submodel scheme is designed based on the sintering process mechanisms and non-uniformity analysis. Then, an adaptive forgetting factor-enabled algorithm is proposed to deal with the time-varying nature in the sintering process with an output of one-minute resolution. After that, the data set is modified according to the system delay analysis, and enriched based on the infrared images of the sintering bed. Finally, implementation and validation of the TS monitoring on a DT system are conducted.

Note to Practitioners—This paper was motivated by the problem of the data-driven sintering process modeling and TS monitoring for a DT system. It also applies to other complex processes in industrial modeling. DT techniques enable the interaction of data between the physical system and the virtual model, which provides a way to update, thus keeping the model accurate in the long term. However, the complex process makes it difficult to design a suitable light-weighted data-driven model scheme with an adaptive update mechanism, to guarantee the operations stable in DT. A model with high computing complexity could lead to DT system collapse when the model cannot return results in real time. This paper suggests a pipeline for constructing a light-weighted data-driven model for a complex process for industrial DT systems. It should be noted that when the DT system contains numerous models, a scheduling strategy for balancing the workloads of multiple models is needed. This paper developed a DT platform scheme with microservice techniques, which can be used for workload balance in future applications. Based on the platform, a TS monitoring service logic diagram is shown for the implementation on a $360m^2$ sintering bed. A three-month result shows that the data-driven model obtains 99.6% monitoring accuracy and achieves a stable workload with a maximum relative standard variance of 7.82%.

Index Terms—Digital twin, Sintering process, Data-driven model, System delay analysis, Machine learning.

I. INTRODUCTION

DIGITAL Twin (DT) is the technique aroused by the development of cloud computing, the Internet of Things (IoT), big data, and artificial intelligence. It has strong potential to improve the productivity as well as optimize the product performance for the complex process industry [1]–[3]. For the DT systems, establishing and verifying accurate physical models is two of the most significant tasks. Constructing a DT system requires knowledge of the production process and interaction between the physical and digital virtual systems [4], [5]. However, due to the complication of the actual production process for industrial process and dispersed data collection of discrete control system (DCS), the effective and stable models for long-term work become the focus of the research [6]–[8].

As a typical industrial process, the sintering process has the characteristics of the complex thermo-chemical reaction, the non-uniformity of materials, system delay, and time-varying. The quality of the sintered ore directly affects the quality of the iron [9], [10]. Moreover, Tumble strength (TS) is one of the critical evaluation indicators of sintering quality [11], [12]. However, the complex process and the lack of timely and continuous monitoring equipment make it difficult to obtain the TS of the sintered ore in real time. Therefore, it is beneficial to establish an accurate TS prediction model and apply the effective DT system to verify the model. Although showing to be significant, the sintering process modeling and online TS monitoring for DT are rarely investigated in the literature.

The sintering process modeling and TS monitoring methods can be categorized into two types, i.e., numerical simulation modeling and data-driven method [13]–[17]. Numerical simulation modeling establishes a mathematical model based on the thermochemical equation in the sintering process under strict constraints and assumptions, whereas performs not well in long-term monitoring due to the time-varying system dynamics [13], [14]. Recently, data-driven models have drawn attention in both academia and industry for their effectiveness in applications. The essence of the TS data-driven model is to train a model based on historical data with the machine learning methods. Based on the input data filtered by correlation analysis, afterwards, Elman neural network, back-propagation neural network, grey neural network, and extreme learning machine (ELM) were used to predict the quality in [18]–[21], respectively. These methods can achieve good monitoring accuracy when the sintering process is time-invariant. Then, the integrated methods were used for sintering modeling to increase monitoring accuracy. A dynamical time-features-expanding and extracting method, along with a

The authors are with the Department of Automation, Shanghai Jiao Tong University, Shanghai, China. E-mails: {dingxuda, yejiale, liu_wei, cailiancehen, xpguan}@sjtu.edu.cn

learning technique, was proposed in [22], where the authors reconstructed the time sequence of input data and then built a data-driven model. Authors in [16] developed an integrated method of ELM and AdaBoost algorithm. The integrated methods increased the model accuracy with complex procedures considering the thermo-chemical process, whereas the computing time of the model was long. To accelerate the computation, authors in [23] proposed a fuzzy neural networks-based method and predicted the quality in two steps, i.e., offline learning and online monitoring. The online monitoring achieved timely computing, which showed the potential for constructing a data-driven model for long-term monitoring. Our previous work [15] considered the non-uniformity of materials characteristics in the sintering process and proposed a data enrichment method for the data-driven model. However, these studies cannot guarantee model accuracy when modeling the time-varying sintering process since they only relied on a pre-sampled offline data set.

Due to the time-varying in the sintering process, the data-driven model cannot cover long-term applications if only a *prior* model construction procedure is performed without updates. Considering the time-varying sintering process, one of the key features of DT systems is data interaction between physical and virtual systems, which provides a way to enable model updates with the online data. Specifically, the data of the sintering process obtained in every minute should be used as a feedback to update the data-driven model. The model can be updated with the actual data to keep up with the varying system continuously for higher modeling accuracy.

However, it is still challenging to construct a sintering process model and monitor online TS value with data interaction in DT. There are three main difficulties. 1) It is difficult to design an effective data-driven scheme for data interaction, and input data selection mechanism for the data-driven model considering the complex thermo-chemical process and the non-uniformity of materials. 2) It is hard to construct a light-weighted model with data interaction to adapt to the time-varying system. The interval between the two consecutive instances of getting monitoring values from the updated data-driven model needs to be smaller than the control periodical interval of the DT system to keep the DT system stable. Thus, the computing time of the online updated TS model is required to be short. 3) Furthermore, the industrial data used for the TS data-driven model construction is incomplete and insufficient [24]. Due to the time delay in the sintering process, the data sampled at time t does not correctly match the exact model at the same time instance. Hereby, directly using these incomplete data as the input of the data-driven model in DT will certainly cause inaccurate results. The data should be processed in the data interaction procedure before used to identify the virtual model in the DT system. On the other hand, the ground truth of TS is insufficient for supervised learning due to the limitation of the monitoring equipment. For example, the actual TS value is obtained every 8 hours, whereas the resolution of the TS data-driven model is one minute. The insufficient data will result in an inaccurate TS model. With the data interaction procedure in DT, an equipment is flexible to be added to the sintering process,

and more data can be obtained for modeling and updating. Enriching the data for accurate modeling and monitoring TS is another issue that needs to be solved.

To tackle these challenges, this paper aims to continuously monitor TS value while keeping the data-driven model adaptive to the time-varying system. In general, the proposed data-driven modeling method provides a lightweight and accurate model, and further guarantees the continuous operation of the DT system. Specifically, we first propose a multi-submodel data-driven scheme to overcome the non-uniformity of materials characteristics in the sintering process, by a designed data interaction procedure in DT to update the model in real time. The input data is selected based on thermo-chemical reaction analysis with the local thermal non-equilibrium (LTNE) model of the sintering process to construct an accurate TS model. Then, a light-weighted data-driven TS model is designed to keep up with the DT system's frequency and the sintering process's time-varying characteristics. We also develop an iterative update algorithm, called Adaptive Forgetting Factor enabled Support Vector Regression (Ada-FFSVR), which effectively avoids frequent retraining for every submodel when new data comes in. The algorithm also realizes continuously monitoring TS value in DT while keeping the data-driven model adapting according to the time-varying system. Furthermore, to construct the data-driven submodels with incomplete and i data, the time delay in the data set is analyzed based on the maximum information coefficient (MIC). Data is enriched by using infrared images of the sintering bed tail for accurate modeling. In general, the proposed scheme and methods provide a methodology of constructing lightweight and accurate data-driven model in real time, and further guarantee the continuous operation of the DT system. The proposed data-driven TS model is implemented on a DT platform for practical application about a sintering process to verify the efficacy of the data-driven model through a three-month operation.

The main contributions of this paper are summarized as follows:

- Considering the non-uniformity of materials characteristics in the sintering process, a multi-submodel data-driven model construction scheme that describes each area of the sintering bed with an update mechanism is proposed. Different submodels represent different areas of the sintering bed to model the non-uniformity of the materials. The scheme constructs an accurate sintering model since it combines the thermo-chemical reaction mechanism of the sintering process and embeds the data interaction of DT to allow the model keep being updated.
- An iterative update algorithm, ada-FFSVR, is proposed for submodels to keep up with the time-varying sintering process. By adding the forgetting factor in the mapping matrix of the submodel, the submodels can iteratively update according to a prescribed threshold triggered by the bias between actual values and model output, for a low computing cost.
- Incomplete and insufficient data is modified and enriched. Time delay is formally analyzed for the time-tagged dataset based on MIC. Data is promised to be aligned to

the same time sequence for model construction and online update in the DT system. The sintering temperature field given by infrared images of the sintering bed tail is used to increase the number of data for constructing a more accurate model. TS value is mapped from the temperature field based on the experiments of the sinter pot test.

- A systemic solution framework for TS data-driven model deploying to the DT system is established and implemented in a practical industrial application. To the best of our knowledge, this is the first work on TS monitoring in the practical DT system. We also show the high long-term monitoring accuracy and low monitoring service workload to validate the efficiency of the proposed model and platform framework.

The paper is organized as follows: The data-driven model scheme and sinter pot test are shown in Section II. The main results of TS modeling analysis, Ada-FFSVR, time delay estimation, and data enrichment with the sinter pot test are given in Section III. In Section IV, we conduct the implementation and application of the TS data-driven model in practice. Section V concludes the paper.

II. DATA-DRIVEN MODEL SCHEME FOR DIGITAL TWIN SYSTEM

A. Descriptions of Sintering Process and Sinter Pot Test

Sintering is a process of forming various types of ore, coke, flux, and other raw materials through heat and pressure to iron-enriched ore. The sintering process is shown in Fig.1, which mainly includes material processing, material sintering, and sintered ore processing stage.

First, in the material processing stage, iron ore, coke, flux, water, and the returning sintered ore are mixed in a particular proportion [25], [26]. The mixture is fed into the sintering

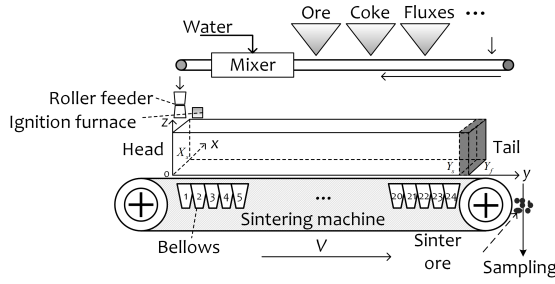


Fig. 1. The demonstration of sintering process

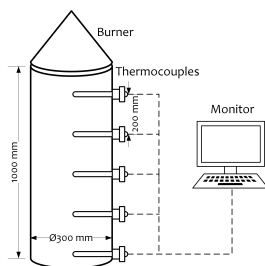


Fig. 2. The demonstration of a sinter pot

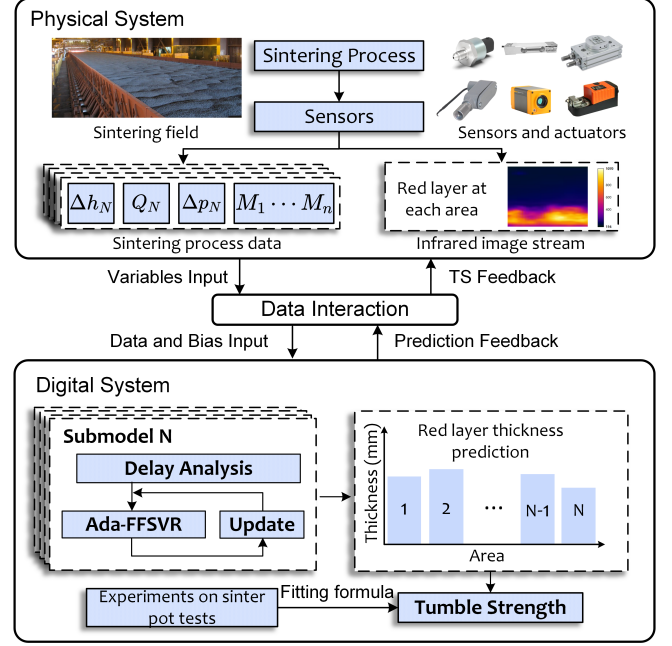


Fig. 3. The data-driven model scheme for DT system

machine through the feeder and the distributor in the material sintering stage. After that, the mixture moves forward with the sintering machine, passes under the igniter, and starts burning. Since the air extraction of the bellows at the sintering machine bottom, the mixture burns from top to bottom. The sintered ore is formulated through a series of physical and chemical reactions. Then, after cooling, crushing, screening, and other operations, the sintered ore can be used for ironmaking.

The complex physical and chemical reactions in the sintering process make it hard to explore the relationship between parameters and quality of the sintered ore. Besides, the continuous production makes onsite experiments extremely dangerous. The sinter pot test is used to simulate the sintering process, verify the theoretical analysis and provide a guidance for practical application [13].

The sinter pot is a cylinder made of heat-resistant steel. The demonstration of the sinter pot is shown in Fig.2. The test procedure is the same as the practical production. In the test, the mixed materials are put into the sinter pot, and the igniter ignites and burns the material thoroughly from the top to the bottom. After the combustion, the sintered ore is formed by cooling, crushing, screening, and other operations.

B. Data-driven Model Scheme

To model the sintering process and online TS monitoring for the DT system, we proposed a data-driven model scheme with the data interaction between the physical and digital systems to connect the two sides. The sintering process data acquired from the sintering field by sensors are used as input variables for data-driven modeling. The number of variables is enormous. It is inefficient to put all the variables into the data-driven model. Thus, the input variables are selected based on the sintering process model mechanism analysis. To consider the non-uniformity of materials in the sintering

bed and obtain accurate TS monitoring, we propose a multi-submodels scheme for the sintering modeling and online TS monitoring in the digital system. Different submodel represents different areas of the sintering bed to model the non-uniformity of materials. The selected data is sent to the submodels for modeling with delay analysis. The delay between input variables is eliminated by aligning the data to the same time sequence. The Ada-FFSVR algorithm is used for training and iteratively updating the data-driven model based on the new input data acquired from the physical system online. By adding the forgetting factor in the mapping matrix of the model, the data-driven model can be sensitive to the new data. The model can iteratively adapt to the new data and operation conditions without a retraining procedure. The update procedure is triggered by bias between the model's output and the actual value enriched by the infrared images. The infrared images indicate the burning temperature field, which is related to the TS value [27]–[29]. The data-driven model directly outputs the temperature field. Next, the fitting formula obtained from experiments on the sinter pot tests maps the outputs from submodels to the TS value with the one-minute resolution. The TS values can be sent back to the physical system as control feedback. Fig.3 shows the scheme of the proposed TS data-driven model.

Remark 1. *The sub-model scheme can introduce more data into the data-driven model. Empirically, more data can increase the model accuracy but the computational complexity at the same time. Thus, the learning algorithm should be lightweight to guarantee that the computing time is short. Furthermore, the number of variables used for learning should be small, and variables should be carefully selected. In practice, we can also use the multi-thread technique to accelerate the computing speed since submodels in our scheme do not depend on each other.*

The detailed results of the sintering process model analysis, Ada-FFSVR algorithm, time delay estimation method, and data enrichment procedure are given in Section III. Here we want to introduce the sinter pot test, which is used to obtain the fitting formula.

III. MAIN RESULTS

The first question to answer in this section is why we use a multi-submodel data-driven scheme to construct the sintering process model. The sintering process model analysis is given to explain this question. Then, the iterative update algorithm is introduced to learn the data-driven model with update strategy. Finally, delay estimation and data enrichment methodologies are shown to modify and enrich incomplete and insufficient data.

A. Sintering Process Model Analysis

A 3D coordinate system describes the sintering bed. In Fig.1, x , y and z represent the width, length, and height of the sintering bed, respectively. The TS of the sintered ore at the sintering bed tail in each area is inconsistent due to the non-uniformity of the mixed materials. TS result is considered

as an integral of TS in all units. Then, $T(t; x, y, z)$ is defined as the TS of the unit at the position (x, y, z) with time-tag t . The TS result at time t can be formulated with consideration of the system delay,

$$TS(t + t_c) = \frac{\int_0^{X_f} \int_{Y_s}^{Y_f} \int_0^{h(t;x,y)} T(t; x, y, z) dx dy dz}{\int_0^{X_f} \int_{Y_s}^{Y_f} \int_0^{h(t;x,y)} dx dy dz}, \quad (1)$$

where t_c is the cooling time, representing the time interval between the hot sintered ore running at the tail of the sintering bed and the cooled sintered ore sampled for testing. Y_f is the tail of the sintering bed. $(Y_f - Y_s)$ represents the length of the ore block used for sampling and testing. $h(t; x, y)$ is the height of the ore block at the coordination (x, y) at time t .

The term $T(t; x, y, z)$ in (1) is related to melting temperature T_m , solid temperature T_s , gas temperature T_g and sintering bed permeability [27]. The term T_m is given according to [28] as

$$T_m = 1380 + 21.22 f_{Al_2O_3} + 3.35 f_{SiO_2} - 1.8 f_{flux}, \quad (2)$$

where $f_{Al_2O_3}$, f_{SiO_2} , f_{flux} are mass fractions of alumina, silica and flux. Equation (2) shows that T_m varies with the ratio of sintering raw materials. Furthermore, T_g and T_s during sintering process is given based on LTNE model as follows [13], [29],

$$\begin{aligned} \varepsilon \cdot c_{p,g} \rho_g \frac{\partial T_g}{\partial \tau} &= \nabla \cdot (\lambda_g \nabla T_g) - \nabla (c_{p,g} \rho_g T_g \nu \cdot \varepsilon) \\ &\quad + h_\nu (T_s - T_g) + R_1 \Delta H_1 + \sum_{i=6}^7 R_i \Delta H_i, \\ (1 - \varepsilon) \cdot c_s \rho_b \frac{\partial T_s}{\partial \tau} &= \nabla \cdot (\lambda_{s,e} \nabla T_s) + h_\nu (T_g - T_s) \\ &\quad - R_1 \Delta H_1 + q_m + \sum_{i=2}^5 R_i \Delta H_i, \end{aligned} \quad (3)$$

where ε is porosity, h_ν is dynamic viscosity, and c is specific heat coefficient under constant pressure. λ is the effective thermal conductivity coefficient. q_m is melting or solidifying heat, and R is the chemical reaction rate. ΔH is the molecular reaction heat, $i(i = 1, 2, 3, 4, 5, 6, 7)$ represent the physical and chemical reactions such as water transfer, coke burning, limestone decomposition, magnetite oxidation, and hematite reduction, respectively.

However, the parameters in (2) and (3) are hard to determine in practical. Feasible substitutions are needed for practical applications. According to [13], $R_i \Delta H_i$, $f_{Al_2O_3}$, f_{SiO_2} , f_{flux} are related to the composition of sintering mixed materials. Parameters ε and h_ν in (3) are related to sintering bed permeability as [30],

$$A_p = \frac{Q}{A} \left(\frac{\Delta h}{\Delta p} \right)^{\frac{3}{5}}, \quad (4)$$

where Q is air volume, A is the bottom area, Δh is the height of the mixed materials, and Δp is the pressure bellows. Then, the TS can be given as

$$TS(t + t_f + t_c) = \frac{\int_0^{X_f} \int_{Y_s}^{Y_f} \int_0^{h(t,t_f;x,y)} g(\cdot) dx dy dz}{\int_0^{X_f} \int_{Y_s}^{Y_f} \int_0^{h(t,t_f;x,y)} dx dy dz}, \quad (5)$$

where $g(\Delta h, Q, \Delta p, M_1, \dots, M_n; x, t) = T(t + t_f; x, y, z)$, $g(\cdot)$ is a nonlinear function. $\Delta h(x; t)$, $\Delta Q(x; t)$ and $\Delta p(x; t)$ are the height of mixed materials, the air volume, and the pressure bellows at the head of the sintering bed with width x at time t , respectively. $M_1(t), \dots, M_n(t)$ are the composition of mixed materials added at time t . Since t is when the mixed materials are added at the head of the sintering bed, the sintering time t_f needs to be added when the batch of mixed material moves to the tail of the sintering bed. For application, we assume that the height of sintered ore at the tail of the sintering bed is constant, and the sampling width is small that the property of ore from (x, Y_s) to (x, Y_f) keeps invariant. Then, (5) can be simplified as

$$TS(t + t_f + t_c) \approx \frac{\sum_{i=1}^N g_i(\Delta h_i, Q_i, \Delta p_i, M_1, \dots, M_n; t) \Delta X}{N}, \quad (6)$$

where $i = 1, 2, \dots, N$ represents each area along the width of the sintering bed, and N represents the total number of areas. Therefore, we can use N submodels to represent TS in each area, considering material non-uniformity in the sintering bed. Note that the submodels are independent of each other. The function $g_i(\cdot)$ is still unknown. The Ada-FFSVR algorithm is then proposed for the data-driven model to learn the function $g_i(\cdot)$.

Remark 2. According to (6), we can obtain $TS(t + t_f + t_c)$ based on $g_i(\Delta h_i, Q_i, \Delta p_i, M_1, \dots, M_n; t)$. Thus, the TS value can be monitored (predicted) in advance of $t_f + t_c$. The current TS value can be obtained based on historical data $(\Delta h_i, Q_i, \Delta p_i, M_1, \dots, M_n; t - t_f - t_c)$. We prefer the term "prediction" when we use the current data to obtain the TS value in advance.

B. Ada-FFSVR with Update Strategy

Consider a function $g_i(x) = \omega_i \phi(x) + b$ to fit the system, where $\phi(\cdot)$ is a nonlinear function mapping x from the original state space into a higher feature space. Then, support vector regression (SVR) is formulated according to [31] as

$$\min_{\omega_i, b} \frac{1}{2} \|\omega_i\|^2, \quad (7a)$$

$$s.t. \quad |y_i - \omega_i \phi(x_i) - b| \leq \epsilon, \quad (7b)$$

where $x_i = (\Delta h_i, Q_i, \Delta p_i, M_1, \dots, M_n; i)$, and y_i is the actual data obtained from the infrared image in DT with delay t_f . ω is the linear mapping, and ϵ is the error. By introducing slack variables ξ_j and ξ_j^* , (7) can be transformed into a quadratic programming problem as

$$\begin{aligned} \min_{\omega_i, b} \quad & \frac{1}{2} \|\omega_i\|^2 + C \sum_{j=1}^n (\xi_j + \xi_j^*), \\ s.t. \quad & \begin{cases} y_i - \omega_i \cdot \phi(x_i) \leq \epsilon + \xi_j, \\ y_i - \omega_i \cdot \phi(x_i) \geq \epsilon + \xi_j^*, \\ \xi_j \geq 0, \\ \xi_j^* \geq 0. \end{cases} \end{aligned} \quad (8)$$

where C is a regularization coefficient. By introducing the Lagrangian dual multipulier α_j, α_j^* , and the Gaussian kernel

function $K(x_j, x)$ in (8), and the function $g_i(x)$ can be obtained [31].

$$g(x) = \sum_{j=1}^n (\alpha_j - \alpha_j^*) K(x_j, x) = \mathbf{K}\boldsymbol{\alpha}. \quad (9)$$

where $\boldsymbol{\alpha}$ is $[\alpha_1 - \alpha_1^*, \alpha_2 - \alpha_2^*, \dots, \alpha_n - \alpha_n^*]^\top$, and \mathbf{K} is $[K(x_1, x), K(x_2, x), \dots, K(x_n, x)]$. Different coefficient α of each submodel represents the non-uniformity in the sintering process. Note that the sintering process is a time-varying system since the operation condition changes with time. Consequently, the output value drastically changes. An initial training procedure cannot meet the long-term accurate prediction requirement. To avoid frequent offline retraining procedure, the Ada-FFSVR algorithm is proposed for iterative changing the support vector coefficient $\boldsymbol{\alpha}$ by the forgetting factor to obtain a more accurate data-driven model timely. When (9) is trained with initial data x_0 , the initial output is y_0 . The variable with the subscript t is its iterative version at time t . The coefficient $\boldsymbol{\alpha}_t$ is updated during the data interaction by the following procedure [32].

$$\boldsymbol{\alpha}_{t+1} = \boldsymbol{\alpha}_t + \frac{\mathbf{L}_{t+1} \mathbf{K}_{t+1}^\top}{1 + \mathbf{K}_{t+1} \mathbf{L}_t \mathbf{K}_{t+1}^\top} e_{t+1}, \quad (10)$$

where the subscript t represents the terms at time t , $e_{t+1} = y_{t+1} - \mathbf{K}_{t+1} \boldsymbol{\alpha}_t$, and $\mathbf{L}_t = (\mathbf{K}_t^\top \mathbf{K}_t)^{-1}$. y_{t+1} is the actual value at $t+1$ and \mathbf{K}_{t+1} is constructed based on input data at $t+1$. To keep the term $\mathbf{K}_t^\top \mathbf{K}_t$ being non-singular, it can be *ad hoc* regularized by adding a small value diagonal matrix [33]. The term $\mathbf{K}_{t+1} \mathbf{L}_t \mathbf{K}_{t+1}^\top$ influences the estimation results, because it is related to the new samples used in the data-driven model. Furthermore, to alleviate the influence of the old sample while increasing the variation caused by the new data, a forgetting factor $1 \geq \gamma > 0$ is added to the \mathbf{L}_t .

$$\mathbf{L}_{t+1} = \mathbf{L}_t - \frac{\mathbf{L}_t \mathbf{K}_{t+1}^\top \mathbf{K}_{t+1} \mathbf{L}_t}{\varepsilon_{t+1}^{-1} + \mathbf{K}_{t+1} \mathbf{L}_t \mathbf{K}_{t+1}^\top}, \quad (11)$$

where

$$\varepsilon_{t+1} = \gamma_t - \frac{1 - \gamma_t}{\xi_{t+1}}. \quad (12)$$

The forgetting factor γ_t is updated according to the new samples matrix \mathbf{K}_{t+1} and the model output error e_{t+1} as

$$\begin{aligned} \gamma_{t+1} = & \{1 + (1 + \varpi)[\ln(1 + \varsigma_{t+1}) \\ & + \left(\frac{(\kappa_{t+1} + 1)\zeta_{t+1}}{1 + \varsigma_{t+1} + \chi_{t+1}} - 1\right) \frac{\varsigma_{t+1}}{1 + \varsigma_{t+1}}]\}^{-1}, \end{aligned} \quad (13)$$

where $\chi_{t+1} = \frac{\varepsilon_{t+1}^2}{\zeta_{t+1}}$, $\zeta_{t+1} = \lambda_t(\zeta_t + \frac{\varepsilon_{t+1}^2}{1 + \xi_{t+1}})$, $\kappa_{t+1} = \lambda_t(\nu_t + 1)$ and $\varsigma_{t+1} = \mathbf{K}_{t+1} \mathbf{L}_t \mathbf{K}_{t+1}^\top$. The term ϖ is a fixed number. Initial values ζ and κ are between 0 and 1.

When the operation changes drastically, the accuracy of the data-driven model decreases [24], [34]. In case of the iterative update no longer guarantees the model accuracy, a retrain strategy needs to be designed. The average error triggers the retrain to keep the update procedure efficient. Specifically, the average error \bar{e} is defined as

$$\bar{e} = \sum_{i=1}^N \frac{1}{N} (g_i(x_i) - y_i). \quad (14)$$

Algorithm 1: Ada-FFSVR algorithm for sub-model

Input: $(\Delta h_i, Q_i, \Delta p_i, M_1, \dots, M_n; i)$, y_i obtained from sintering field, parameters ϖ, ζ, κ and ϵ .
Output: The prediction $g_i(x_i)$.

```

1 Use initial data set to train SVR and obtain  $K_0\alpha_0$ ;
2  $t = 0$ ;
3 Compute  $g_i(x_0)$  according to (9);
4 while true do
5   Construct  $K_{t+1}$  based on  $t + 1$ -th samples;
6   Obtain  $L_{t+1}$  according to (11), (12) and (13);
7   Compute  $\alpha_{t+1}$  according to (10);
8   Obtain  $g_i(x_{t+1})$  according to (9);
9   Calculate  $\bar{e}$  according to (14);
10  if  $\bar{e} \geq \epsilon$  then
11    Select new sample to retain the SVR and
        obtain  $K_{t+1}\alpha_{t+1}$ ;
12    Compute  $g_i(x_{t+1})$  according to (9);
13  end
14   $t = t + 1$ .
15 end
```

where $g_i(\cdot)$ is the fitting function of the sub-model, x_i is the input data, and y_i is the benchmark output. A threshold $\epsilon > 0$ triggers the update procedure. When $\bar{e} \geq \epsilon$, the model is retrained with new data set. The new data set is selected by substituting the samples whose errors are higher than the threshold for the samples with the smallest value in the Lagrange equation of (8).

The proposed algorithm does not need a frequent retrain procedure because of its iteration design of a threshold. This guarantees the stability of the DT system when the model update. The number of training samples of the algorithm is always the same in this study, and the size of the matrix of the model keeps unchanged, which helps keep a low computational cost. The Algorithm of Ada-FFSVR with a retraining strategy is shown in Algorithm 1.

C. Delay Estimation and Data Enrichment

According to (9) and (10), matrix K is constructed based on data sampled from the sintering process. Since the system delay is in the process, the same time-tagged data may not correctly match the model sequence. Moreover, the delay is unknown. To construct a suitable dataset, the delays between the samples need to be estimated and eliminated.

The main idea for time delay analysis is to analyze the correlation of two sequences of variables under different time lags. Mutual information (MI) is an effective tool to analyze the correlation between two variables [35]. When the MI between the two sequences reaches the maximum at a certain time lag, the two variables have the strongest correlation at this time lag, and then it is a specific time delay between the two variables [24].

Suppose there are two time series of variables, $x_i^n = \{x_i, x_{i+1}, \dots, x_{i+n}\}$, $y_i^n = \{y_i, y_{i+1}, \dots, y_{i+n}\}$ represent n observation sample sequence of X and Y at i -th time, respectively. A finite set of ordered pairs of X and Y under time lag

k is $D_{i,k}^n = \{(x_i, y_{i+k}), (x_{i+1}, y_{i+1+k}), \dots, (x_{i+n}, y_{i+n+k})\}$. Given a grid G which partitions the x -values of $D_{i,k}^0 \in \mathbb{R}^2$ into x bins and y -values of $D_{i,k}^0$ into y bins. The estimation of MI between two variables with a delay of k is given as:

Lemma 1. *The Maximal Information Coefficient (MIC) of $D_{i,k}^0$ with sample size n and grid size less than $B(n)$ is given as [36]*

$$M(D_{i,k}^0) = \max_{xy < B(n)} \left\{ \frac{\max I(D_{i,k}^0 | G)}{\log \min\{x, y\}} \right\}, \quad (15)$$

where $D_{i,k}^0 | G$ is the distribution induced by the points in $D_{i,k}^0$ on the cells of G . The term $I(D_{i,k}^0 | G)$ denotes the MI of $D_{i,k}^0 | G$. $\omega(1) < B(n) \leq O(n^{1-\varepsilon})$, $0 < \varepsilon < 1$.

Then, to identify the time delay between X and Y , the sliding window method [24] is adopted. The time delay τ between X and Y can be obtained according to

$$\begin{aligned} & \arg \max_{\tau} \{M(D_{i,\tau}^n)\}, \\ & \text{s.t. } \tau \in \mathbb{Z}. \end{aligned} \quad (16)$$

When τ is the time delay between X and Y , the MIC of $D_{i,\tau}^n$ is the largest term among $\{M(D_{i,0}^n), M(D_{i,1}^n), \dots, M(D_{i,k}^n)\}$, $k \in \mathbb{Z}$. The sign of τ provides the direction of the time delay between variables X and Y . If τ is positive, the direction of the delay is from variable Y to X , i.e., X lags behind Y . When τ is negative, the direction is from variable X to variable Y , i.e., Y lags behind X .

Remark 3. *In practice, the sampling frequencies of variables are sometimes inconsistent. For example, the sampling period of the height of mixed materials is one minute, and that of TS is eight hours. The difference in sampling frequencies makes the time delay cannot be analyzed directly by the proposed method since the data densities are not the same. Therefore, frequency matching of the two variables is required. To unify the frequency, the data with high frequency is re-sampled under the low frequency. This way, the sample data sets of two variables are the same size, and the time delay can be analyzed based on the proposed method.*

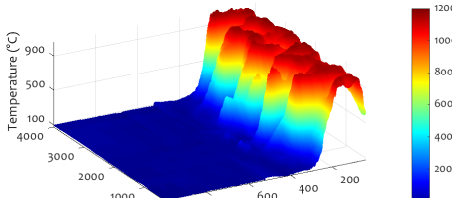
The sequence of variables is adjusted according to time delay τ , which is identified based on (16). Define $\tilde{x}_i^n, \tilde{y}_i^n$ as the adjusted variables for x_i^n, y_i^n , respectively. The sequences of variables are displaced to be stacked as

$$\begin{aligned} \tilde{x}_i^n &= \{x_i, x_{i+1}, \dots, x_{i+n}\}, \\ \tilde{y}_i^n &= \{y_{i+\tau}, y_{i+1+\tau}, \dots, y_{i+n+\tau}\}. \end{aligned} \quad (17)$$

Since the actual value of TS cannot be obtained every minute to examine whether the update should be triggered, the intermedia variable is introduced into the data-driven model as the learning algorithm output. Motivated by existing studies on the relationship between burning temperature field and TS [27]–[29], we introduce the data based on the infrared image of the sintering bed tail section and sinter pot test results, to enrich the actual value, so that the update procedure is efficient.



(a) Infrared image



(b) Temperature distribution

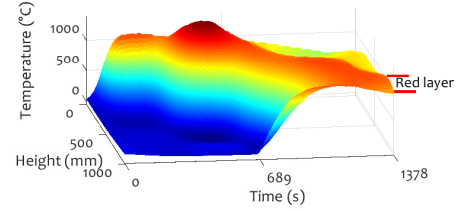
Fig. 4. Infrared image and temperature distribution at the sintering bed tail

The infrared images show the combustion pattern of the sintered ore at the sintering bed tail section. The TS is related to the thickness of the red layer, i.e., the ore whose temperature is above 1000°C. Then, the sinter pot test results connect the sinter quality and the thickness of the red layer. Fig.4 shows the infrared images and the temperature distribution of the materials on the $x - z$ plane in (6). Fig.4 (a) is the infrared image with a resolution of 640×480 collected by infrared camera, and Fig.4 (b) is the temperature distribution of materials on the the $x - z$ plane in (6). The thickness of the red layer can be easily obtained from the infrared image. The sinter pot tests are conducted to obtain the right formula, to regress the relationship between thickness and TS [15]. The temperature in the sinter pot can be directly obtained through 5 thermocouples, and then the TS of the sintered ore is obtained by manual detection. Fig.5 (a) shows the temperature fluctuations of a sinter pot test, and Fig.5 (b) shows the temperature field changing in the sinter pot and the demonstration of the red layer. Based on sinter pot tests, the fitting formula is obtained as [15]:

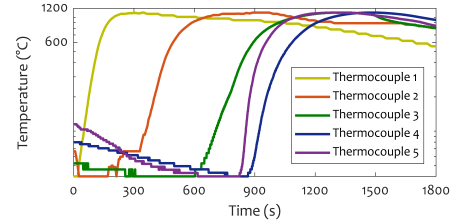
$$\theta = 16.8891 \ln(\vartheta) - 17.6491, \quad (18)$$

where θ represents the thickness of the red layer (mm), ϑ represents the TS (%).

So far, the TS data-driven model has been established. First, through the data of input variables collected by the sensors in each area of the sintering bed along the width, monitoring (prediction) of the thickness of the red layer is obtained based on Ada-FFSVR with an update strategy. The average output of the submodels is used for a further calculation, which corresponds to the integration in (6). Then, the value of the TS can be calculated according to the fitting formula between the thickness of the red layer and the TS obtained by the sinter pot test. Finally, we get TS in (6) by averaging the results. Considering the uneven distribution of mixed materials in the model scheme, the data-driven model is accurate and practical for applications. Ada-FFSVR, with an update strategy, further



(a) Temperature distribution in a sinter pot



(b) Thermocouple temperature in the sinter pot

Fig. 5. Temperature distribution in the sinter Pot

considers the time-varying characteristics of the sintering process. The proposed data-driven model scheme combines the sintering mechanism and the learning methods, which endows the potential to increase the model accuracy.

IV. IMPLEMENTATION AND VERIFICATION

To realize the practical application of the online TS monitoring (prediction), we design the sintering DT system and implement the proposed model in the system. The services can be developed based on the platform and provide information for sintered ore production and management, including TS value prediction. There are two requirements for the DT platform:

- The DT platform needs to provide an operating and management environment for the models. The appropriate technical architecture and implementation methods should be proposed for the model construction methodology and specific operational requirements.
- Based on the DT platform and the models, components that provide services for the DT system need to be constructed to constitute the DT system. Specifically, sintering TS prediction components based on DT data-driven model are developed for the application.

A. DT platform for Sintering

The implementation of the DT system relies on numerous models, which further form DT service components and provide services for the DT system through model integration and data interaction. The operation and management of the models depend on a unified platform called the *DT platform*. The relationship between the DT-related modules is illustrated in Fig.6.

Since the models are constructed independently from each other and provide at least one service for the DT system, the model construction method coincides with the idea of micro-services. Micro-services are different from monolithic

TABLE I
LIST OF VARIABLES USED FOR THE DATA-DRIVEN MODEL

NO.	Variables	Positions of Measure points	Role in the Data-driven Model	Sampling Interval
1	The height of mixed materials (6 measure points)	Evenly distributed at the head of the sintering bed		
2	The air volume of the bellow (2 measure points)	Distributed at two sides of the head of the sintering bed	Input	
3	The air pressure of the bellow (2 measure points)	Distributed at two sides of the head of the sintering bed		one minute
4	The weight of raw material (17 measure points)	Located at each raw material storage (including ore, coke, flux, etc.)		
5	The thickness of red layer (6 processed points from image)	Images from the tail of the sintering bed	Intermediate output	
6	TS value (one measure point)	Located at sintered ore storage away from the sintering bed	Output	eight hours

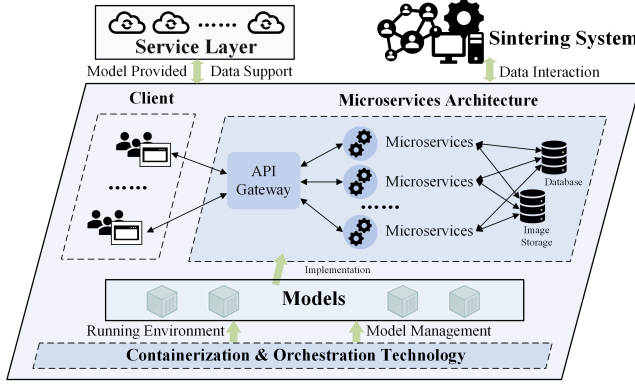


Fig. 6. The relationship between DT modules

applications. The latter is to develop and deploy all application functions together. Although the architecture of monolithic applications has been optimized in load balancing, it still owes problems such as poor fault tolerance, low scalability, and rare development collaboration [37]. Also, micro-services divide an application into several small service modules. Each service is deployed independently and runs independently in its process [37]. The services communicate, coordinate, and cooperate through lightweight communication protocols. Therefore, it is reasonable to build the DT platform for sintering based on the micro-service architecture. We use Harbor to store Docker images and Rancher to implement the Kubernetes function and manage images to construct a DT platform [38]–[40].

B. Application of TS Prediction

To verify the proposed TS data-driven model, the DT platform is established with a TS prediction service for a $360m^2$ sintering bed in Guangxi, China. Verification is applied to the TS model to evaluate its performance in TS prediction. To illustrate the results and comparisons, four services are constructed for visualization in the front-end website. Specifically, the online TS prediction micro-service is the core module of the quality prediction service. The online TS prediction micro-service uses the latest real-time data to predict the

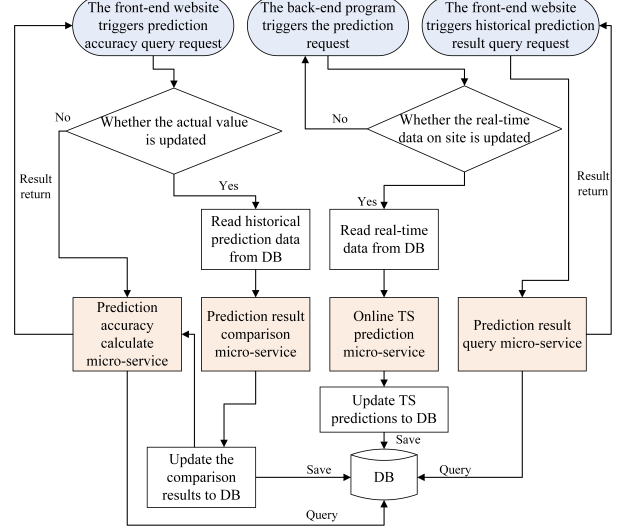


Fig. 7. Logic diagram of TS prediction service

TS and writes the prediction value to the database. At the same time, the query service queries the latest prediction values in nearly two hours from the database and displays the prediction information to users in time. Furthermore, to show the prediction accuracy to users, when the actual value is updated, the prediction accuracy calculates the micro-service calculates the relative error between the prediction value and the actual value. The prediction value and actual value of the past week are displayed to the user for comparison through the prediction result comparison micro-service. The service logic diagram of sintering TS prediction is shown in Fig.7.

1) *Result in TS Prediction:* In this part, the data-driven model is established and used to monitor (predict) long-term TS value. A total of 1,305,600 samples in 38,400 sample sets from approximately 27 days of data are used to train, update and test the model. It should be noted that the actual TS value is sampled three times a day, and we select 80 samples of the actual TS value to show the prediction error of the data-driven model. Table I. shows the variables used for the data-driven model. The initial data-driven model uses the first 300 sets of samples for training, and a 5-fold cross-validation grid searching optimizes parameters. Then, we select the initial

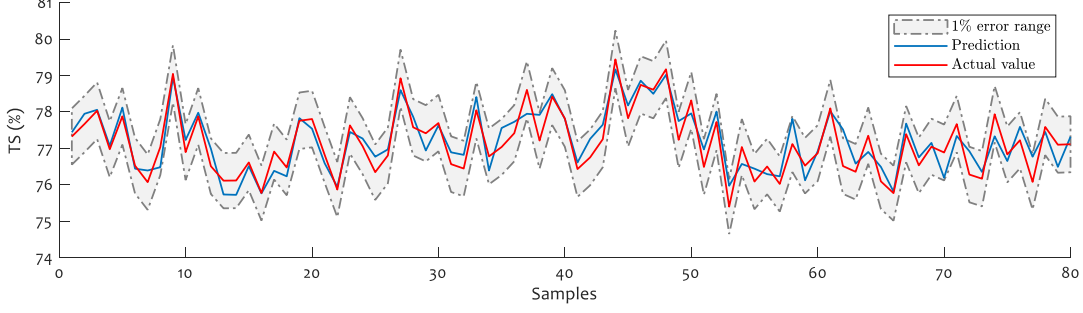


Fig. 8. Long-term prediction of TS value for about 27 days

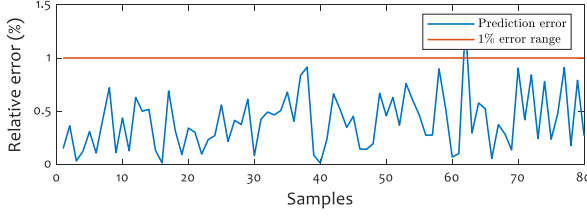


Fig. 9. Long-term prediction error of TS value for about 27 days

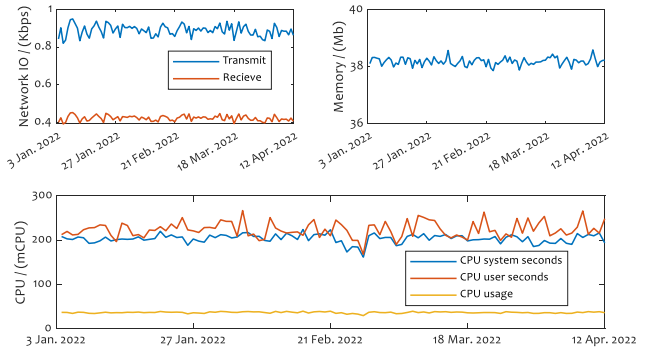


Fig. 10. Long-term workload of online TS prediction micro-service

parameter $\gamma_0 = 0.1$, $\zeta_0 = 1$, $\kappa_0 = 0.1$, $\varpi = 20$ in Ada-FFSVR, and $\epsilon = 0.01$ in the update procedure. Fig. 8 shows the long-term prediction of TS value based on the proposed data-driven model and DT platform. Fig. 9 shows the prediction relative error of TS value. The results show that the proposed data-driven model is effective, and 98.75% of the prediction values has a relative error below 1%. Statistical results, namely root mean square error (RMSE), mean relative error (MRE), normalized mean square error (NMSE), and Pearson correlation coefficient (R), were used to evaluate the accuracy of the model. The values of error parameters are

calculated as follows:

$$\begin{aligned} \text{RMSE} &= \sqrt{\frac{1}{m} \sum_{i=1}^m (y_i - \hat{y}_i)^2}, \\ \text{MRE} &= \frac{1}{m} \sum_{i=1}^m \frac{|y_i - \hat{y}_i|}{y_i}, \\ \text{NMSE} &= \frac{\sum_{i=1}^m (y_i - \hat{y}_i)^2}{\sum_{i=1}^m y_i^2}, \\ R &= \frac{\sum_{i=1}^m (y_i - \bar{y})(\hat{y}_i - \bar{\hat{y}})}{\sqrt{\sum_{i=1}^m (y_i - \bar{y})} \sqrt{\sum_{i=1}^m (\hat{y}_i - \bar{\hat{y}})}}, \end{aligned}$$

where y_i , \hat{y}_i , \bar{y} and $\bar{\hat{y}}$ are the actual value, the predicted value, the average actual value and the average of predicted value, respectively. The term m is the size of the sample set. Table. II shows the statistical results, the number of update times, and the longest update computing time of the proposed data-driven model. As a comparison, the results in [15]–[17] are also shown in Table II. RMSE, MRE, and NMSE of the prediction based on the proposed method are smaller than those based on the methods in the literature. The term R of the prediction based on the proposed method is also larger compared to these methods. The statistical results show that the proposed data-driven model is more accurate and effective. Regarding model prediction accuracy, 98.75% of the prediction results based on the proposed method are within 1% of the relative

TABLE II
STATISTICAL RESULTS OF TS PREDICTION BASED ON DIFFERENT METHODS

	Method in [16]	Method in [17]	Method in [15]	Our method
RMSE (%)	0.74	-	0.48	0.37
MRE (%)	0.74	< 3.50	0.51	0.40
NMSE	-	0.34	-	2.30×10^{-5}
R	0.84	0.81	-	0.91
Update frequency ¹	-	-	-	3.39×10^{-2}
The longest computing time (s) ²	-	-	-	23.58

¹ The update frequency is the ratio of the total update times and the number of sample sets.

² The longest computing time used for the retraining.

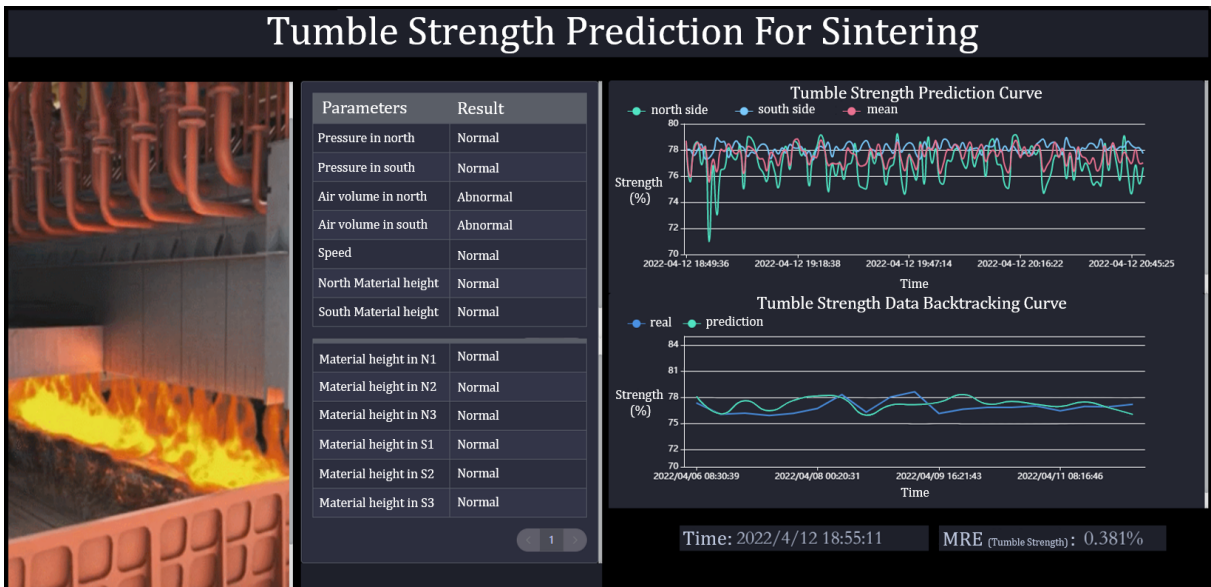


Fig. 11. Front-end website of TS prediction service in DT

error, and the maximum relative error is only 1.23%, which satisfies the requirement of the practical application. The update frequency is 3.39×10^{-2} , which illustrates that the data-driven model updates occasionally. The average update interval is about 30 min. The longest computing time of the update is 23.58s, which is smaller than the sampling interval (i.e., one min). Therefore, the proposed data-driven model can timely predict accurate results and meet the actual industry operation requirements.

2) Result in TS Prediction Service: The online prediction micro-service is established based on the proposed data-driven model. The prediction accuracy micro-service, the comparison micro-service, and the results query micro-service are constructed to illustrate the prediction results (see Fig. 7). The online prediction micro-service consumes the immense workload on CPU, network, and memory among the constructed micro-services since it continuously predicts the TS results and automatically updates the model.

Fig. 10 shows the workload of prediction micro-service in 99 days. The network I/O, memory, and CPU workloads of the online TS prediction micro-service keep stable for a long time, which shows that 1) the proposed data-driven model is light-weighted and efficient; 2) the proposed architecture

of the DT platform effectively manages the micro-services without breakdowns in a long-term operation. The maximum relative standard variance of the workload is 7.82 %, which shows the efficiency of the proposed platform. The stability of the operation is critical for industry operation and the DT platform. The breakdown of a DT micro-service could lead to system-level failure since the micro-service is essential and provides basic data for other services.

Fig. 11 and Fig. 12 show the application of TS prediction and DT platform onsite. The DT platform provides information about the TS and sintering quality for the operators onsite (see Fig. 12). Fig. 11 is the shot cut of the front-end website of the TS prediction service. We showed the north-side, the south-side and the mean predictions on the screen. The prediction results, accuracy, and comparisons are shown on the right side of the front-end website, which is powered by micro-services. The left side of the website shows a picture of the sintering site. The middle of the website shows the fault diagnosis results, which is beyond the scope of this paper.

V. CONCLUSION

This paper developed a multi-submodel data-driven TS model for the sintering DT system with data interaction. The modeling includes multi submodel scheme, TS model mechanism analysis, and Ada-FFSVR algorithm with an update strategy to deal with non-uniformity material and time-varying characteristic in the sintering process. We also introduced a system-delay-estimation-based data set modification and an infrared image-based data enrichment procedure to deal with incomplete and insufficient data for constructing a data-driven TS model. A concrete systematic solution for implementing and applying TS value monitoring in the DT platform is given to illustrate the detailed development procedure. A three-month operation for a sintering bed in Guangxi, China, is performed to show the efficiency of the data-driven TS model.



Fig. 12. Operators use TS prediction and DT platform

Despite the advantages of the proposed method demonstrated above, it also has some limitations that need to be studied in future research. 1) The TS value is given based on the fitting formula. In general, the sintering material used for sintered ore production is stable for long term in practice. The fitting formula can cover the long-term operation condition. When the material changes drastically, it requires an update mechanism for the formula. 2) The proposed method aims to build a stable and accurate model, which is the basis for a stable DT system. The stability and efficiency of the entire DT system depend on stable and accurate models and a systematic scheduling strategy for workload balancing. In conclusion, a systematic scheduling strategy for the DT system to keep the functional operation is another interested problem to be studied in the future.

REFERENCES

- [1] Y. Li, C. Yang, H. Zhang, and J. Li, "Discussion on key technologies of digital twin in process industry," *ACTA AUTOMATICA SINICA*, vol. 47, no. 3, p. 14, 2021.
- [2] M.-H. Hung, Y.-C. Lin, H.-C. Hsiao, C.-C. Chen, K.-C. Lai, Y.-M. Hsieh, H. Tieng, T.-H. Tsai, H.-C. Huang, H.-C. Yang, et al., "A novel implementation framework of digital twins for intelligent manufacturing based on container technology and cloud manufacturing services," *IEEE Transactions on Automation Science and Engineering*, 2022.
- [3] T. Wang, J. Cheng, Y. Yang, C. Esposito, H. Snoussi, and F. Tao, "Adaptive optimization method in digital twin conveyor systems via range-inspection control," *IEEE Transactions on Automation Science and Engineering*, 2020.
- [4] A. Rasheed, O. San, and T. Kvamsdal, "Digital twin: Values, challenges and enablers from a modeling perspective," *IEEE Access*, vol. 8, pp. 21980–22012, 2020.
- [5] G. Shao and M. Helu, "Framework for a digital twin in manufacturing: Scope and requirements," *Manufacturing Letters*, vol. 24, pp. 105–107, 2020.
- [6] Q. Min, Y. Lu, Z. Liu, C. Su, and B. Wang, "Machine learning based digital twin framework for production optimization in petrochemical industry," *International Journal of Information Management*, vol. 49, pp. 502–519, 2019.
- [7] F. Tao, H. Zhang, A. Liu, and A. Y. Nee, "Digital twin in industry: State-of-the-art," *IEEE Transactions on Industrial Informatics*, vol. 15, no. 4, pp. 2405–2415, 2018.
- [8] Y. Zheng, S. Yang, and H. Cheng, "An application framework of digital twin and its case study," *Journal of Ambient Intelligence and Humanized Computing*, vol. 10, no. 3, pp. 1141–1153, 2019.
- [9] S. Du, M. Wu, L. Chen, K. Zhou, J. Hu, W. Cao, and W. Pedrycz, "A fuzzy control strategy of burn-through point based on the feature extraction of time-series trend for iron ore sintering process," *IEEE Transactions on Industrial Informatics*, vol. 16, no. 4, pp. 2357–2368, 2019.
- [10] P. Zhou, S. Zhang, L. Wen, J. Fu, T. Chai, and H. Wang, "Kalman filter-based data-driven robust model-free adaptive predictive control of a complicated industrial process," *IEEE Transactions on Automation Science and Engineering*, vol. 19, no. 2, pp. 788–803, 2021.
- [11] J. An, J. Yang, M. Wu, J. She, and T. Terano, "Decoupling control method with fuzzy theory for top pressure of blast furnace," *IEEE Transactions on Control Systems Technology*, vol. 27, no. 6, pp. 2735–2742, 2018.
- [12] J. Liu, J. He, Z. Tang, Y. Xie, W. Gui, T. Ma, H. Jahanshahi, and A. A. Aly, "Frame-dilated convolutional fusion network and gru-based self-attention dual-channel network for soft-sensor modeling of industrial process quality indexes," *IEEE Transactions on Systems, Man, and Cybernetics: Systems*, 2021.
- [13] B. Zhang, J. Zhou, and M. Li, "Prediction of sinter yield and strength in iron ore sintering process by numerical simulation," *Applied Thermal Engineering*, vol. 131, pp. 70–79, 2018.
- [14] Z. Cheng, J. Yang, L. Zhou, Y. Liu, and Q. Wang, "Sinter strength evaluation using process parameters under different conditions in iron ore sintering process," *Applied Thermal Engineering*, vol. 105, pp. 894–904, 2016.
- [15] J. Ye, X. Ding, C. Chen, X. Guan, and X. Cao, "Tumble strength prediction for sintering: Data-driven modeling and scheme design," in *2020 Chinese Automation Congress (CAC)*, pp. 5500–5505, IEEE, 2020.
- [16] S. Wang, H. Li, Y. Zhang, and Z. Zou, "A hybrid ensemble model based on elm and improved adaboost. rt algorithm for predicting the iron ore sintering characters," *Computational intelligence and neuroscience*, vol. 2019, 2019.
- [17] T. Umadevi, D. Naik, R. Sah, A. Brahmacharyulu, K. Marutiram, and P. Mahapatra, "Studies on parameters affecting sinter strength and prediction through artificial neural network model," *Mineral Processing and Extractive Metallurgy*, vol. 125, no. 1, pp. 32–38, 2016.
- [18] Q. Wang and Q. Liu, "Research on online prediction of sinter quality based on elman neural network," *Instrument Technique and Sensor*, no. 10, p. 25, 2017.
- [19] X. Fan, Y. Li, and X. Chen, "Prediction of iron ore sintering characters on the basis of regression analysis and artificial neural network," *Energy Procedia*, vol. 16, pp. 769–776, 2012.
- [20] J. Zhang, A. Xie, and F. Shen, "Multi-objective optimization and analysis model of sintering process based on bp neural network," *Journal of Iron and Steel Research International*, vol. 14, no. 2, pp. 1–5, 2007.
- [21] Z. Li, X. Fan, G. Chen, G. Yang, and Y. Sun, "Optimization of iron ore sintering process based on elm model and multi-criteria evaluation," *Neural Computing and Applications*, vol. 28, no. 8, pp. 2247–2253, 2017.
- [22] Y. Li, C. Yang, and Y. Sun, "Dynamic time features expanding and extracting method for prediction model of sintering process quality index," *IEEE Transactions on Industrial Informatics*, vol. 18, no. 3, pp. 1737–1745, 2021.
- [23] M. J. Er, J. Liao, and J. Lin, "Fuzzy neural networks-based quality prediction system for sintering process," *IEEE Transactions on Fuzzy Systems*, vol. 8, no. 3, pp. 314–324, 2000.
- [24] Y. Zhai, X. Ding, X. Jin, and L. Zhao, "Adaptive lssvm based iterative prediction method for nox concentration prediction in coal-fired power plant considering system delay," *Applied Soft Computing*, vol. 89, p. 106070, 2020.
- [25] L.-H. Hsieh, "Effect of raw material composition on the sintering properties," *ISIJ international*, vol. 45, no. 4, pp. 551–559, 2005.
- [26] D. Fernández-González, I. Ruiz-Bustinza, J. Mochón, C. González-Gasca, and L. F. Verdeja, "Iron ore sintering: Process," *Mineral Processing and Extractive Metallurgy Review*, vol. 38, no. 4, pp. 215–227, 2017.
- [27] C. E. Loo, N. Tame, and G. C. Penny, "Effect of iron ores and sintering conditions on flame front properties," *ISIJ international*, vol. 52, no. 6, pp. 967–976, 2012.
- [28] N. K. Nath and K. Mitra, "Optimisation of suction pressure for iron ore sintering by genetic algorithm," *Ironmaking & steelmaking*, vol. 31, no. 3, pp. 199–206, 2004.
- [29] B. Alazmi and K. Vafai, "Analysis of fluid flow and heat transfer interfacial conditions between a porous medium and a fluid layer," *International Journal of Heat and Mass Transfer*, vol. 44, no. 9, pp. 1735–1749, 2001.
- [30] E. Voice, S. Brooks, and P. Gledhill, "The permeability of sinter beds," *Journal of the Iron and Steel Institute*, vol. 174, pp. 136–139, 1953.
- [31] V. Vapnik, *The nature of statistical learning theory*. Springer science & business media, 1999.
- [32] J. Mendes, R. Araújo, and F. Souza, "Adaptive fuzzy identification and predictive control for industrial processes," *Expert Systems with Applications*, vol. 40, no. 17, pp. 6964–6975, 2013.
- [33] J. L. Rojo-Álvarez, M. Martínez-Ramón, M. de Prado-Cumplido, A. Artés-Rodríguez, and A. R. Figueiras-Vidal, "Support vector method for robust arma system identification," *IEEE transactions on signal processing*, vol. 52, no. 1, pp. 155–164, 2004.
- [34] W. Wang, C. Men, and W. Lu, "Online prediction model based on support vector machine," *Neurocomputing*, vol. 71, no. 4–6, pp. 550–558, 2008.
- [35] C. E. Shannon, "A mathematical theory of communication," *The Bell system technical journal*, vol. 27, no. 3, pp. 379–423, 1948.
- [36] D. N. Reshef, Y. A. Reshef, H. K. Finucane, S. R. Grossman, G. McVean, P. J. Turnbaugh, E. S. Lander, M. Mitzenmacher, and P. C. Sabeti, "Detecting novel associations in large data sets," *science*, vol. 334, no. 6062, pp. 1518–1524, 2011.
- [37] N. Dragoni, S. Giallorenzo, A. L. Lafuente, M. Mazzara, F. Montesi, R. Mustafin, and L. Safina, "Microservices: yesterday, today, and tomorrow," *Present and ulterior software engineering*, pp. 195–216, 2017.
- [38] A. M. Potdar, D. Narayan, S. Kengond, and M. M. Mulla, "Performance evaluation of docker container and virtual machine," *Procedia Computer Science*, vol. 171, pp. 1419–1428, 2020.

- [39] S. Buchanan, J. Rangama, and N. Bellavance, "Deploying and using rancher with azure kubernetes service," in *Introducing Azure Kubernetes Service*, pp. 79–99, Springer, 2020.
- [40] O. Mironov, "Devops pipeline with docker," 2018.



Xuda Ding (S'20) received the B.E. and M.E. degrees in School of Automation from North China Electric Power University, China, in 2016 and 2019. He is working toward a Ph.D. with the Department of Automation, Shanghai Jiao Tong University, Shanghai, China. He is a member of the Intelligent of Wireless Networking and Cooperative Control group. His research interests include data-driven modeling, safety-critical control, and digital twin system in industrial applications.



Cailian Chen (M'06) received the B.E. and M.E. degrees in Automatic Control from Yanshan University, P. R. China in 2000 and 2002, respectively, and the Ph.D. degree in Control and Systems from City University of Hong Kong, Hong Kong SAR in 2006. She joined the Department of Automation, Shanghai Jiao Tong University, in 2008 as an Associate Professor. She is now a Full Professor. Before that, she was a postdoctoral research associate at the University of Manchester, U.K. (2006–2008). She was a Visiting Professor at the University of Waterloo, Canada (2013–2014). Prof. Chen's research interests include industrial wireless networks, computational intelligence and situation awareness, and the Internet of Vehicles.

Prof. Chen has authored three research monographs, and over 100 referred international journal papers. She is the inventor of more than 20 patents. She received the prestigious "IEEE Transactions on Fuzzy Systems Outstanding Paper Award" in 2008 and the Best Paper Award of WCSP17 and YAC18. She won the Second National Natural Science Award from the State Council of China in 2018, the First Prize of Natural Science Award from The Ministry of Education of China in 2006 and 2016, respectively, and the First Prize of Technological Invention of Shanghai Municipal, China in 2017. She was honored Changjiang Young Scholar in 2015 and Excellent Young Researcher by NSF of China in 2016. Prof. Chen has been actively involved in various professional services. She is Associate Editor of IEEE Transactions on Vehicular Technology, Puerto-peer Networking, and Applications (Springer). She also served as Guest Editor of IEEE Transactions on Vehicular Technology, TPC Chair of ISAS19, Symposium TPC Co-chair of IEEE Globecom 2016 and VTC2016-fall, and Workshop Co-chair of WiOpt18.



Jiale Ye received the B.E. degree in the College of Energy and Power Engineering, Nanjing University of Aeronautics and Astronautics, Nanjing, China, in 2019, and the M.E. degree in the Department of Automation, Shanghai Jiao Tong University, Shanghai, China, in 2022.



Xinping Guan (F'18) received the B.S. degree in Mathematics from Harbin Normal University, Harbin, China, in 1986, and the Ph.D. degree in Control Science and Engineering from Harbin Institute of Technology, Harbin, China, in 1999. He is currently a Chair Professor with Shanghai Jiao Tong University, Shanghai, China, where he is the Dean of the School of Electronic, Information and Electrical Engineering and the Director of the Key Laboratory of Systems Control and Information Processing, Ministry of Education of China. Before that, he was the Professor and Dean of Electrical Engineering at Yanshan University, Qinhuangdao, China.

Dr. Guan's current research interests include industrial cyber-physical systems, wireless networking and applications in smart factories, and underwater networks. He has authored and/or coauthored five research monographs, more than 270 papers in IEEE Transactions and other peer-reviewed journals, and numerous conference papers. As a Principal Investigator, he has finished/been working on many national key projects. He is the leader of the prestigious Innovative Research Team of the National Natural Science Foundation of China (NSFC). Dr. Guan is an Executive Committee Member of the Chinese Automation Association Council and the Chinese Artificial Intelligence Association Council. Dr. Guan received the First Prize of Natural Science Award from the Ministry of Education of China in both 2006 and 2016 and the Second Prize of the National Natural Science Award of China in both 2008 and 2018. He was a recipient of the IEEE Transactions on Fuzzy Systems Outstanding Paper Award in 2008. He is a National Outstanding Youth honored by NSF of China, Changjiang Scholar by the Ministry of Education of China, and State-level Scholar of New Century Bai Qianwan Talent Program of China.



Wei Liu received the B.E. degree from Fuzhou University, Fuzhou, China, and the M.E. degree from Xiamen University, Xiamen, China, in 2014 and 2017, respectively. He is working toward a Ph.D. in engineering with the Department of Automation, Shanghai Jiao Tong University, Shanghai, China. He is working in the Intelligent Wireless Network and Cooperative Control group. His current research interests include data-based modeling, quality monitoring, and machine learning.